ISSN 1063-7826, Semiconductors, 2015, Vol. 49, No. 3, pp. 309–312. © Pleiades Publishing, Ltd., 2015.
Original Russian Text © V.A. Novikov, D.V. Grigoryev, 2015, published in Fizika i Tekhnika Poluprovodnikov, 2015, Vol. 49, No. 3, pp. 319–322.

SURFACES, INTERFACES, AND THIN FILMS

Investigation of Surface Potential in the *V*-Defect Region of MBE $Cd_xHg_{1-x}Te$ Film

V. A. Novikov^ and D. V. Grigoryev

Tomsk State University, Tomsk, 634050 Russia

^e-mail: novikovvadim@mail.ru

Submitted April 8, 2014; accepted for publication June 3, 2014

Abstract—Atomic-force microscopy is used to investigate the distribution of the contact-potential difference (surface potential) in $Cd_xHg_{1-x}Te$ epitaxial films grown by molecular-beam epitaxy. Modification of the solid-solution composition near the *V*-defect results in a variation in the contact-potential difference. It is shown that the solid-solution composition varies by ~0.05 (2.5 at %) towards increasing mercury content in the *V*-defect region, and a region of mercury depletion by 0.36 at % is observed at the *V*-defect periphery. From analysis of the surface-potential distribution, it is shown that the $Cd_xHg_{1-x}Te$ epitaxial film contains unform *V*-defects with a diameter less than 1 μm in addition to macroscopic *V*-defects.

DOI: 10.1134/S106378261503015X

1. INTRODUCTION

The ternary semiconductor compounds $Cd_xHg_{1-x}Te$ (CMT), where the material composition x is the molar content of Cd, are the basic materials for the fabrication of IR (infrared) intrinsic photodetectors in the wavelength range of 3–5 and 8–14 μm [1]. Heteroepitaxial CMT films grown by molecular-beam epitaxy (MBE) are the most promising materials for the fabrication of multielement photoreception devices (MPRDs) of infrared radiation providing processing of the signal directly in the focal region. One of the main problems in the fabrication of highly efficient MPRDs is the obtainment of high uniformity of sensitive matrix elements in the focal plane. Hence, it is necessary to attain a high degree of uniformity of the composition and structural perfection of the CMT epitaxial films [2]. As was shown in [3–5], the greatest effect on the uniformity of the working characteristics of matrix elements in the focal plane is exerted by *V*-defects. These defects are formed during the growth of epitaxial films on substrates with an orientation differing from (111) and (100). The size of these defects amounts to 5–20 μm. *V*-defects represent a polycrystal, the sizes of the individual crystallites of which vary from 0.5 to 1.5 μm, and the height varies from 0.3 to 1.0 μm [6].

In studies devoted to investigating the composition of a ternary solution in the *V*-defect region, it is shown that this defect can contain an excess of mercury, cadmium, or tellurium. In [3, 7], it was concluded from X-ray spectral analysis that a tellurium excess as large as 3% occurs in the region of an epitaxial film with a high *V*-defect concentration. At the same time, experimental data obtained by the method of electron-probe X-ray microanalysis show that an increase in the mercury content by 6 at % [6] is observed in the *V*-defect region. Thus, determination of the composition of the ternary solution in the *V*-defect region is an urgent problem.

2. EXPERIMENTAL

In these investigations, we used heteroepitaxial *p*-CMT films grown by the MBE method on GaAs substrates of the (013) orientation with ZnTe and CdTe buffer layers [2]. The epitaxial structures were grown at the IPS, Siberian Branch, Russian Academy of Sciences, Novosibirsk. After growth, the film had *n*-type conductivity. For conversion to *p*-type conductivity, the films were annealed in a neutral atmosphere of hydrogen or helium [2].

The surface-potential distribution was investigated by the Kelvin probe force microscopy (KPFM) using a Solver HV atomic-force microscope (AFM) (made by NT-MDT, Zelenograd) under normal conditions. We used probes based on boron-doped polycrystalline silicon coated with platinum (the probe type is NSGll/Pt, made by NT-MDT).

The KPFM represents the double-passage mode of scanning. On the first pass, we measured the surface morphology; then, the probe was removed from the sample surface at a set distance (10–50 nm) and measured the contact-potential difference (CPD) at each scanning point. To determine the CPD between the needle tip and the sample, dc and ac voltages are applied. The measurements are performed at the first harmonic of the ac bias. As a result, an electric force arises between the sample surface and the cantilever-needle tip, which depends on the capacitance in the

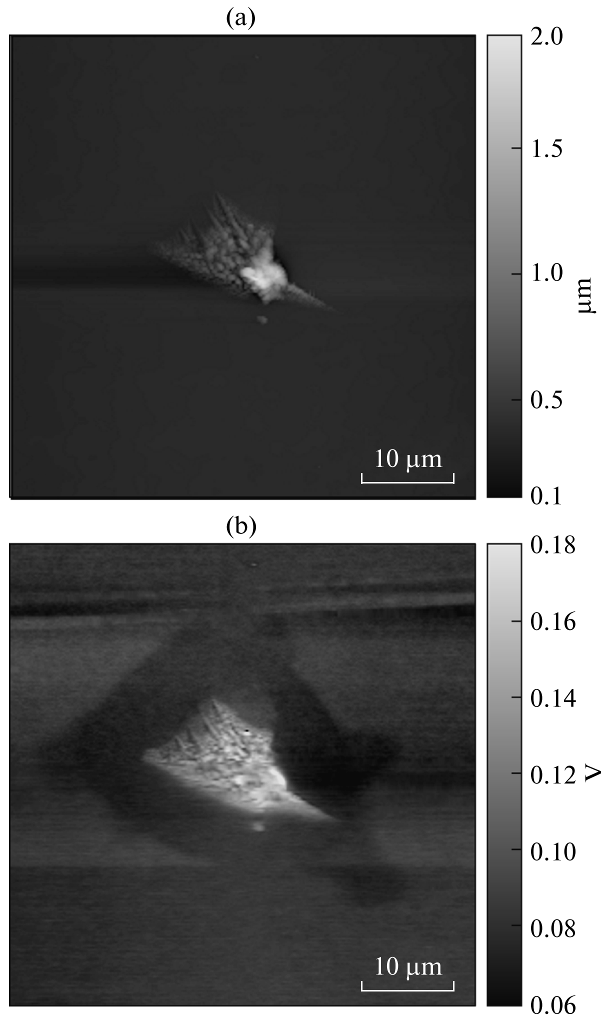

Fig. 1. (a) AFM image of a *V*-defect in $Cd_xHg_{1-x}Te$; (b) the CPD distribution in the *V*-defect region of $Cd_xHg_{1-x}Te$.

probe-tip–sample-surface gap, the dc voltage, and the induced potential:

$$F(\omega) = -[V_{dc} - V_{cp} + V_{ind}]V_{ac}\sin(\omega t)\frac{dc}{dz}, \qquad (1)$$

where V_{dc} is the dc voltage applied between the probe and the sample; V_{cp} is the surface potential; V_{ind} is the potential induced in the surface region; and $V_{ac}\sin(\omega t)$ is the ac bias. From expression (1), it can be seen that, keeping the force under measurement equal to zero, the value of the applied bias is $V_{dc} = V_{cp} - V_{ind}$ and, since the material does not change, the CPD oscillations over the sample surface only depend on the value of V_{cp}, i.e., on the modification of the electrical properties of the surface region of the CMT epitaxial film.

Variation in material composition (x) on the epitaxial-film surface results in modification of the electronic properties of the surface region. Hence, this modification can be detected by determining the contact-potential difference (surface potential) via the KPFM. This method finds wide application for investigating the distribution of the built-in [8] and external potentials in device-oriented microstructures and nanostructures [9–11]. Therefore, in this study, the KPFM was used to investigate the surface-potential distribution over the surface of the CMT epitaxial film.

3. RESULTS

In Fig. 1, we show typical AFM images of the surface morphology and the distribution of CPD in the *V*-defect region of the $Cd_xHg_{1-x}Te$ epitaxial film. From Fig. 1b, it can be seen that, in the region of this defect, an increase in the CPD with respect to that in the basic matrix of the material is observed. The CPD variation amounts to ~70 mV. Along the *V*-defect periphery, we observed a potential halo with an insignificant (about 10 mV) decrease in the CPD value.

As was mentioned above, the CPD variation is determined by that of the surface potential, which, in turn, depends on the difference in the work functions of the probe and the sample [12]. Since the work function of a solid solution depends on the composition of the CMT epitaxial film, the spatial distribution of the surface potential can be associated with the variation in the solid solution.

The work function of the AFM probe remains invariable during measurement. Using the linear approximation for the work function of the $Cd_xHg_{1-x}Te$ solid solution (the work function amounts to 4.5 eV for CdTe and 5.9 eV for HgTe [13]), we write the expression for the variation in the CPD in the *V*-defect region in the following form:

$$\Delta CPD = V_{cp} - V_{ind} = \varphi_2 - \varphi_1 - V_{ind}, \qquad (2)$$

considering that V_{ind} is independent of the solid-solution composition (this assumption is permissible because the CPD oscillations are small, and the solid-solution composition varies insignificantly), and the work function of the solid solution is $\varphi_i = x_i\,\varphi_{CdTe} - (1 - x_i)\varphi_{HgTe}$, it is possible to write the expression for determining the change in the CMT solid-solution composition in the following form:

$$x_2 = \frac{\Delta CPD}{\varphi_{CdTe} - \varphi_{HdTe}} + x_1. \qquad (3)$$

From analysis of the CPD distribution in the *V*-defect region, we obtained $\Delta CPD \approx 70$ mV; then taking into account expression (3), the solid-solution composition should vary by 0.05 towards an increasing mercury content, which well coincides with the results reported in [6].

The potential halo with the smaller CPD corresponds to a decreasing mercury content in this region ($|\Delta x| \approx 0.025$–0.007). The width of the mercury-

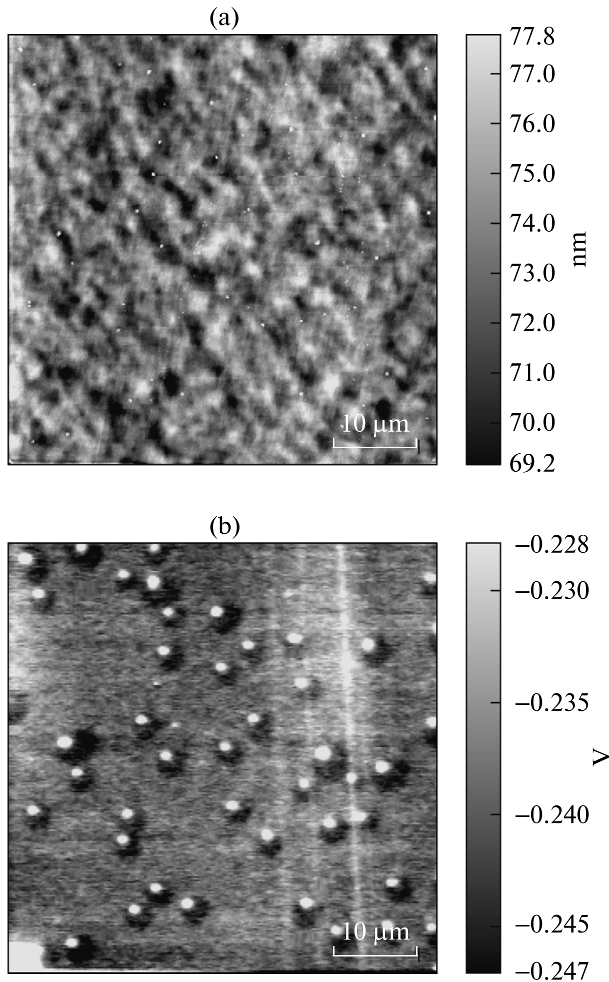

Fig. 2. (a) AFM image of the surface morphology in $Cd_xHg_{1-x}Te$; (b) CPD distribution in $Cd_xHg_{1-x}Te$.

depletion region amounts to about 10 μm. We observed local broadening of the potential halo in the region of acute angles of the *V*-defect. This broadening, presumably, is related to a local increase in mercury outflow for the formation of *V*-defect crystallites.

In Fig. 2, we show the data of AFM measurements of the surface morphology and the CPD distribution beyond the *V*-defect region. The surface roughness at a scanning-area width of 50 μm and number of scanning points of 256 amounts to 1.5 nm. On the surface, we observed hills 5–10 nm in height and 0.5–1 μm in basis diameter.

From Fig. 2b, it can be seen that, for a fraction of these hills, the distribution of the contact-potential difference is similar to the distribution observed for *V*-defects up to the presence of the peripheral region depleted of mercury. From comparison of the CPD distribution in the *V*-defect region and beyond it, we can assume that the CMT epitaxial film contains also unform *V*-defects of round shape in addition to only macroscopic *V*-defects. Analysis of the CPD distribution shows that the variation in the composition in the region of unform defects is approximately two times lower than in the *V*-defect region.

From Fig. 2b, it can also be seen that the centers of the mercury-depleted regions are displaced in one direction instead of being arranged at the defect center. This displacement is less than 1 μm; therefore, it is practically undetected in the CPD distribution in the *V*-defect region. In our opinion, it is related to the fact that *V*-defects and, consequently, also unform *V*-defects grow through at an angle of 68.58° to the (310) plane [14, 15].

4. CONCLUSIONS

In this study, we investigated the CPD distribution in $Cd_xHg_{1-x}Te$ epitaxial films grown by the MBE method. It is experimentally shown that, in the *V*-defect region, an increase in the contact-potential difference by about 70 mV is observed. At the *V*-defect periphery, we observed a region with an insignificant (about 10 mV) decrease in the CPD value, which forms a potential halo. It was shown that variations in the spatial distribution of the CPD are associated with a variation in the local composition of the CMT epitaxial-film material. Analysis of the obtained experimental data showed that *V*-defects are distinguished by an increased mercury content, which is in agreement with the results obtained in [6]. At the *V*-defect periphery, a mercury-depletion region (the potential halo) is observed, the width of which amounts to about 10 μm. In this case, local broadening of the potential halo is observed in the region of acute angles of the *V*-defect. This broadening, presumably, is associated with a local increase in the mercury outflow for the formation of *V*-defect crystallites.

Investigation of the spatial distribution of the surface potential beyond the *V*-defect region showed the presence of defects less than 1 μm in diameter on the surface of the material, the distribution of the contact potential difference of which is similar to that observed for *V*-defects. The variation in the composition in the region of unform *V*-defects is approximately two times less in comparison with macroscopic *V*-defects; however, their concentration is much higher.

ACKNOWLEDGMENTS

We thank N.N. Mikhailov and V.S. Varavin for supplying us with the MBE samples of CMT epitaxial films for the investigations.

The study is supported within the framework of the Program of increasing competitiveness of the National Tomsk State Research University.

REFERENCES

1. A. Rogalski, *Infrared Detectors* (CRC, Boca Raton, 2000; Nauka, Novosibirsk, 2003).
2. V. N. Ovsyuk, G. L. Kuryshev, Yu. G. Sidorov, et al., *Matrix Photodetectors in Infrared Region* (Novosibirsk, Nauka, 2001) [in Russian].
3. Yu. G. Sidorov, S. A. Dvoretsky, V. S. Varavin, et al., Semiconductors **35**, 1045 (2001).
4. I. V. Sabinina et al., J. Cryst. Growth **117**, 238 (1992).
5. E. V. Permikina, A. S. Kashuba, and I. A. Nikiforov, Usp. Prikl. Fiz. **1**, 510 (2013).
6. A. S. Kashuba, A. V. Zablotskii, E. V. Korostylev, et al., Vestn. MITKhT **5**, 19 (2010).
7. S. N. Yakunin and N. N. Dremova, JETP Lett. **87**, 494 (2008).
8. C.-S. Jiang, H. R. Moutihno, D. J. Friedman, J. F. Geisz, and M. M. Al-Jassim, Appl. Phys. Lett. **93**, 10035 (2003).
9. A. V. Ankudinov, A. N. Titkov, R. Laiho, and V. A. Kozlov, Semiconductors **36**, 1058 (2002).
10. A. Doukkali, S. Ledain, C. Guasch, and J. Bonnet, Appl. Surf. Sci. **235**, 507 (2004).
11. Kl.-D. Katzer, W. Mertin, and G. Bacher, Appl. Phys. Lett. **89**, 103522 (2006).
12. N. A. Torkhov and V. A. Novikov, Semiconductors **43**, 1071 (2009).
13. A. Zozime and C. Vermeulin, Rev. Phys. Appl. **23**, 1825 (1988).
14. I. V. Sabinina, A. K. Gutakovsky, Yu. G. Sidorov, and A. V. Latyshev, J. Cryst. Growth **274**, 339 (2005).
15. V. V. Arbenina, A. S. Kashuba, and E. V. Permikina, Vestn. MITKhT **8**, 82 (2013).

Translated by V. Bukhanov